LTR Control Methodologies for Microvibrations

G. S. Aglietti[1], J. Stoustrup[2], E. Rogers[1], R. S. Langley[3], and S. B. Gabriel[1]

1: Dept Aero. and Astro/
Dept Elect. and Comp. Science
Univ. of Southampton, UK
etar@ecs.soton.ac.uk

2: Dept Control Engineering
Aalborg University
Denmark

3: Dept Engineering
University of Cambridge
UK

Abstract

Microvibrations at frequencies between 1 and 1000 Hz generated by on-board equipment can propagate through a satellite's structure and hence significantly reduce the performance of sensitive payloads. This paper describes a Lagrange-Rayleigh-Ritz method for developing models suitable for the design of active control schemes. Here Loop Transfer Recovery based controller design methods are employed with this modeling strategy.

1 Introduction

Recent years have seen a dramatic increase in the stability requirements placed on payload instruments, with consequent increases in the level of vibration suppression demanded from the spacecraft structure. As a result, low amplitude vibrations at frequencies between 1 Hz and 1000 Hz, generally termed microvibrations, once neglected due to the low levels of disturbances induced on-board satellites, are now of critical importance and are the subject of much research effort aimed at developing efficient techniques for their control, eg [1]. In effect, such vibrations are produced by the functioning of on-board equipment such as reaction wheels, gyroscopes, thrusters, electric motors etc which propagate through the satellite structure towards sensitive equipment (receivers) thereby jeopardizing their correct functioning.

Vibration suppression requirements are particularly demanding for micro-gravity experiments and accurately targeted optical instruments. Included in the latter class are mirror pointing systems, such as those found on space telescopes where small mechanical disturbances produce jitter which can result in severe blurring of the images collected by these systems. Also in this class are interferometers where the optical path difference must be controlled to nanometer accuracy. In other equipment, such as laser communications systems, vibration induced oscillations of the beam causes problems at the receiving station.

In practice, the reduction of the vibration level onboard satellites is attempted by action at the source(s), receiver(s), and along the vibration path(s). At the source(s), this action consists of attempting to minimize the amplitude of the vibration(s) by, for example, placing equipment on appropriate mountings. The same approach is commonly attempted at the receiver(s) but with the basic objective of sensitivity reduction. Finally, along the vibration path(s), modifications of structural elements or relocation of equipment is attempted with the aim of reducing the mechanical couplings between sources and receivers.

All of the approaches described above are based on so-called passive damping technology and, for routine applications, an appropriate combination of them is often capable of producing the desired levels of dynamic disturbance rejection. The use of active control techniques in such cases would only be as a last resort to achieve desired performance. In the case of microvibrations, however, only active control can be expected to provide the required levels of suppression.

To investigate the use of active control to suppress microvibrations, computationally feasible models which retain the core features of the underlying dynamics are clearly required. The most obvious approach to the development of such models is to use finite element methods (FEM) due to the accuracy available with a sufficiently fine mesh. The only difficulty with this approach is the computational intensity of the models in terms of their subsequent use for control systems design and evaluation (eg closed loop simulation studies). They can, however, be used, as here, to verify that the modeling strategy employed produces 'realistic' models on which to base controller design and evaluation.

Alternatives to FEM, can be classified as elastic wave methods, variational methods, and mechanical impedance based methods respectively. A detailed study of the advantages and disadvantages of these methods can be found in [2]. Based on this study, a Lagrange-Rayleigh-Ritz (LRR) method is used to develop the mathematical models used as a basis for the controller design studies reported in this paper.

A key feature of the LRR approach is that the resulting models can be immediately written in state space form for robust controller design and evaluation. Here the use of this modeling procedure to design Loop Transfer Recovery (LTR) based controllers is illustrated.

2 System Description and Modeling

Equipment on-board satellites is often mounted on lightweight panels where microvibrations have to be suppressed to achieve the desired level of performance. Here we restrict attention to one such mass loaded panel - an acceptable compromise between problem complexity and the need to gain useful insights into the benefits (and limitations) of active control schemes in this general area. A schematic diagram of the arrangement considered is shown in Figure 1, where the equipment mounted on the panel is modeled as lumped masses and the disturbances as point forces.

The sensors and actuators employed in this work are twin patches of piezoelectric material bounded onto opposite faces of the panel. The bending vibrations of the plate produce stretching and shrinking of the patches depending on whether they are on the top or the bottom of it (Figure 2a). Due to the piezoelectric effect, these deformations induce an electric field perpendicular to the plate which is detected by the electrodes of the patches. The outer electrodes of the patches are electrically connected together and the plate, which is grounded, is used as the other electrode for both patches of the pair. The same configuration is used for the actuator, but in this case the electric field is applied externally to produce contraction or expansion of the patch, which then induces a curvature of the plate.

A key point is that the effectiveness of the piezoelectric elements, both as actuators and sensors, is significantly reduced if the wavelength of the deformations is smaller than the patch. The essential reason for this reduced effectiveness is that the signal produced in this case is partially or completely (as in Figure 2b) cancelled by the opposing field generated by the other part of the patch as it is deformed in the opposite direction. This limiting factor is especially important when attempting to control high frequency vibrations which have, of course, very short wavelengths. One possible means of increasing the effectiveness of the patches in these situations would be to increase the patch dimension, but care is needed since this would also diminish the control authority at low frequencies.

The LRR based procedure used to model this system (Figure 1) is based on Lagrange's equations of motion

which in the general case take the form

$$\frac{d}{dt}(\frac{\partial T}{\partial \dot{q}_i}) - \frac{\partial T}{\partial q_i} + \frac{\partial U}{\partial q_i} = Q_i \qquad (1)$$

Here T and U are the kinetic and potential energies of the system, and q_i and Q_i are the ith generalized coordinate and force respectively. For the particular case of Figure 1, the kinetic and potential energies (elastic and electric) can be expressed as

$$\begin{aligned} T &= T_{pl} + T_{lm} + T_{pz} \\ U &= U_{pl} + U_{pz_{elast}} + U_{pz_{elastelect}} + U_{pz_{elect}} \end{aligned} \qquad (2)$$

where T_{pl}, T_{lm} and T_{pz} denote the kinetic energies of the plate, lumped masses, and piezoelectric patches respectively, U_{pl} is the elastic energy stored in the plate, $U_{pz_{elast}}$ is the elastic energy stored in the piezoelectric patches, $U_{pz_{elastelect}}$ represents the potential energy due to the voltage driven piezoelectric effect, and $U_{pz_{elect}}$ is the electric energy stored due to the dielectric characteristics of the piezoelectric material.

The displacement field (out-of-plane displacement w) is described by a superposition of shape functions $S_{m,n}$ (consisting of the first $Nm.Nn$ modes of the bare panel) multiplied by the time dependent modal co-ordinates $\phi_{m,n}$, i.e.

$$w(x,y,t) = \sum_{m=1}^{Nm} \sum_{n=1}^{Nn} S_{m,n}(x,y)\phi_{m,n}(t) = s^T \Phi \qquad (3)$$

where the $Nm.Nn \times 1$ column vectors s and Φ contain the shape functions and modal co-ordinates respectively.

The external excitation consists of Nf point forces F_j acting on the plate at arbitrary locations. Hence the generalized forces are of the form

$$Q_i = \sum_{j=0}^{Nf} F_j \frac{\partial w}{\partial \phi_i} \text{ or } Q = S_f f \qquad (4)$$

where f is the Nf $\times$ 1 column vector of forces and S_f is a compatibly dimensioned matrix whose columns are given by the model shape vector s evaluated at the corresponding force locations.

It is now necessary to compute each of the terms in (2), starting with the kinetic energies. Each of these terms can be calculated using standard formulas [2]. Their final forms in terms of the corresponding inertia matrices are given by

$$T_{pl} = \frac{1}{2}\dot{\Phi}^T M_{pl}\dot{\Phi}, \ T_{pz} = \frac{1}{2}\dot{\Phi}^T M_{pz}\dot{\Phi}, \ T_{lm} = \frac{1}{2}\dot{\Phi}^T M_{lm}\dot{\Phi} \qquad (5)$$

The potential energy of the system is stored as the elastic energy of the plate and the elastic/electric energy

of the piezoelectric patches. In the case of the plate, use of a standard formula [2] gives

$$U_{pl} = \frac{1}{2}\Phi^T K_{pl}\Phi \qquad (6)$$

where K_{pl} is the plate stiffness matrix. Also, by assuming a linear strain pattern across the piezoelectric patches, the same procedure for the plate can be used to write

$$U_{pz_{elast}} = \frac{1}{2}\Phi^T K_{pz_{elast}}\Phi \qquad (7)$$

where is the stiffness matrix which is fully populated and can be computed by using a standard formula as detailed in [2].

The additional stress which arises in the ith piezoelectric patch when an electric field $e_i(t) = v^T(t)p_i$ (where v is the column vector containing the Np patch voltages, and the column vector p_i has zero entries except for $\frac{1}{h_{pz_i}}$ (inverse of the patch thickness) in the ith position is applied across the material can be expressed as (E_{pz} Young's modulus, ν Poisson's ratio)

$$\sigma_{elect} = \begin{pmatrix} \sigma_{x_{elect}} \\ \sigma_{y_{elect}} \end{pmatrix} = \frac{E_{pz}}{1-\nu^2}\begin{pmatrix} d_{xz} + \nu d_{yz} \\ d_{yz} + \nu d_{xz} \end{pmatrix} e_i \quad (8)$$

Here d_{xz} and d_{yz} are the piezoelectric constants of the material, which is assumed to have pole direction z perpendicular to the plate. This additional stress, multiplied by the assumed strain, defines $U_{pz_{elastelect}}$ which can be calculated by substituting (8) into the expression

$$U_{pz_{elastelect}} = \frac{1}{2}\int\int\int_{pz_i} \sigma_{elect}^T \epsilon\, dx\, dy\, dz \qquad (9)$$

where pz_i denotes the volume of the ith patch.

By assuming $d_{xz} = d_{yz} = d_z$ it is possible to write the elastoelectric energy stored in the Np patches as

$$U_{pz_{elastelect}} = v^T K_{pz_{elastelect}}\Phi \qquad (10)$$

where $K_{pz_{elastelect}}$ can be computed as explained in [2]. Also the electrical energy stored in the piezoelectric material can be expressed as

$$U_{pz_{elect}} = \frac{1}{2}\int\int\int_{pz_i} e\, d\, dx\, dy\, dz \qquad (11)$$

where e is the electric field and d is the electric displacement (charge/area). For each patch, the electric displacement is

$$d_i = \epsilon_{pz_i} p_i^T v \qquad (12)$$

where ϵ_{pz_i} is the dielectric constant of the piezoelectric material which forms the ith patch. Hence an equivalent expression for the stored electric energy is

$$\begin{aligned} U_{pz_{elect}} &= \frac{1}{2}v^T K_{pz_{elect}} v \\ K_{pz_{elect}} &= \sum_{i=1}^{Np}\int\int\int_{pz_i} \epsilon_{pz_i} p_i p_i^T\, dx\, dy\, dz \end{aligned} \quad (13)$$

where the elements of the matrix $K_{pz_{elect}}$ are the capacitances of the piezoelectric patches.

At this stage, all of the energy terms are available as functions of the generalized co-ordinates Φ and v. Hence it is a straightforward task to apply Lagrange's equations of motion (1). This is again detailed in [2] and hence only the final result is given here.

The most general case arises when some of the patches act as actuators and others as sensors. In which case it is necessary to partition the matrix $K_{pz_{elastelect}}$ to separate out actuator and sensor contributions. To do this, let v_a and v_s be the sub-vectors of the voltages at the actuators and sensors respectively, and $K_{pza_{elastelect}}$ and $K_{pzs_{elastelect}}$ the corresponding partitions of $K_{pz_{elastelect}}$. Then by use of (1) we have

$$M\ddot{\Phi} + C_s\dot{\Phi} + (K_{elas} + K_{pzs})\Phi = -K_{pza_{elastelect}}^T v_a + s_f^T f \qquad (14)$$

where all inertia elements are included in the matrix M and all stiffness elements in the matrix K_{elas}. Also

$$K_{pzs} = -K_{pzs_{elastelect}}^T K_{pzs_{elect}}^{-1} K_{pzs_{elastelect}} \qquad (15)$$

represents the contribution to the stiffness from the piezoelectric energy stored in the patches acting as sensors, where $K_{pzs_{elect}}$ is the sub-matrix of $K_{pz_{elect}}$ corresponding to the sensors. The presence of the term $C_s\dot{\Phi}$ also means that damping has been introduced into the overall system.

As an essential step before accepting a model derived by this procedure as a realistic basis for controller design/evaluation studies, appropriate model validation studies must be undertaken. This aspect has been reported in [2] where the basic approach is to compare the results produced by this procedure for a range of structural and input/output configurations against those produced using standard FE models constructed (in this work) using the commercially available software ANSYS.

In the FE model, only the elastic characteristics of the patches were directly modeled with the piezoelectric effects simulated by extrapolating in two dimensions the mono-dimensional theory discussed in [2]. Three different classes of tests were performed, the first of which compared the the output displacement produced by a corresponding input voltage(eg 1 volt) at a patch acting as an actuator. In the FE model for this test, the applied voltage was replaced by a line moment along the patch edges.

The second set of tests, the displacement response of the plate (with a lumped mass added) to point forces was examined. In the third class of tests, the outputs (i.e. voltages) at the sensor in response to point forces was compared. During these tests, the voltages at the

sensor were evaluated from the curvature of the plate at the edges of the patches.

By way of examples, Figure 3 shows a typical response from the first test and Figure 4 a typical response from the second test. In depth analysis all of the results obtained confirms that the modeling technique used here is a viable alternative to other approaches with the added advantage of being a suitable basis for active control studies. The next section proceeds to use this approach to design and evaluate LTR controllers.

3 Control System Design and Evaluation

The model of (14) can easily be written in state space form as follows

$$
\begin{aligned}
\dot{x} &= Ax + B_v u + B_f f \\
v_s &= C_v x \\
w_{out} &= C_w x
\end{aligned}
\tag{16}
$$

where $x = \left[\Phi^T, \dot{\Phi}^T \right]^T$ and, in particular,

$$
C_v = \left[\begin{array}{cc} -K^{-1}_{pzs_{elect}} K_{pzs_{elastelect}} & 0 \end{array} \right] C_w = \left[\begin{array}{cc} s^T_{out} & 0 \end{array} \right]
\tag{17}
$$

Here w_{out} is the output displacement and s_{out} is the vector of mode shapes evaluated at the output location. Using this state space description, it is possible to begin in depth investigations of the potential (or otherwise) of active control schemes in this general area. In this paper the control objective considered is to minimize the displacement at a specified point on the panel in the presence of point force disturbances acting at other location(s) on the panel. The control strategy is based on LTR.

The LTR design methodology followed [3] is the definition of a target feedback loop (TFL) which is then recovered through an asymptotic design. In particular, we follow the well known two step design procedure for recovery at the input of a square plant and its dual for recovery at the plant output. The actual designs were undertaken in MATLAB and Figure 5 shows the resulting system for recovery at the plant output, where L denotes the Kalman filter gain matrix defined by appropriate selection of the covariance matrices W and V. The design is then completed by solving a standard LQR problem with state and control weighting matrices Q and R respectively and is only guaranteed to work for minimum phase plants.

If the plant has non-minimum phase zeros then the recovery procedure may still work provided these zeros lie beyond the desired operating bandwidth. The application here is characterized by non-colocated sensors and actuators and hence the resulting plant transfer func-

tion (or transfer function matrix) could well be non-minimum phase. Below we report one case in detail which shows that LTR design is still possible to some extent in this general area.

The example used here is a particular case of Figure 1 (for the parameters see [2]) where the disturbance is a harmonic point force of 1N amplitude acting perpendicular to the panel and the first 36 modes were taken as Ritz functions to model the displacement field. As expected, this system is non-minimum phase and hence, at best, only a limited degree of LTR is possible. Iterating through the design procedure showed that this was indeed the case for weighting matrices of the form

$$
W = B_f B_f^T, \ V = I, \ Q = C_w^T C_w + qI, \ R = I
\tag{18}
$$

and varying the scalar q upwards from zero to approximately 10^{-2}.

Extensive simulation studies were carried out using the weighting matrices structure just outlined and Figure 6 gives a representative set of results from these studies. This shows the displacement response at the center of the plate without (continuous line) and with (dashed line) control. As a very 'basic robustness' test, the model used in controller design used the first 4 Ritz functions and the simulation results shown are for the same controller applied to a model constructed using the first 6 Ritz functions. It is clear that a good level of vibration reduction has been introduced into the system.

4 Conclusions

This paper has outlined a modeling procedure which can be used to directly construct state space models on which to base active control design studies for the suppression of microvibrations. Here the use of this procedure has been demonstrated by its use to design LTR based controllers. At best, this work has only demonstrated the potential of this modeling strategy, and active feedback control schemes in this general area and clearly much work remains to be done, both on LTR and other robust controller design methodologies.

References

[1]   H. R. Stark, and C. Stavrinidis, "ESA Microgravity and Microdynamics Activities - An Overview", Acta Astronautica, 34, pp.205-221, 1994.

[2]   G. S. Aglietti, "Active Control of Spacecraft Microvibrations", Research Report, Dept Aeronautics and Astronautics, University of Southampton, UK, 1996.

[3]   J. M. Maciejowski, "Multivariable Feedback Design", Addison Wesley, 1989.

Fig. 1. Model layout.

a)   b)
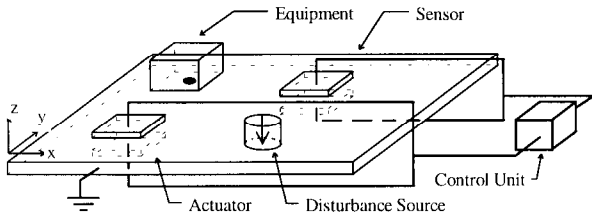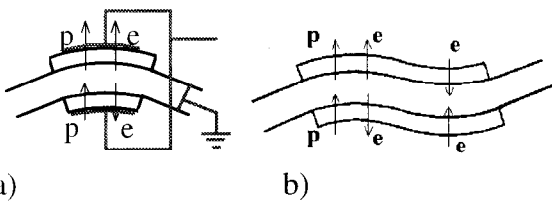
Fig. 2. Patch section view during deformation
a) deformation wavelength longer then patch
b) deformation wavelength equal or shorter then patch
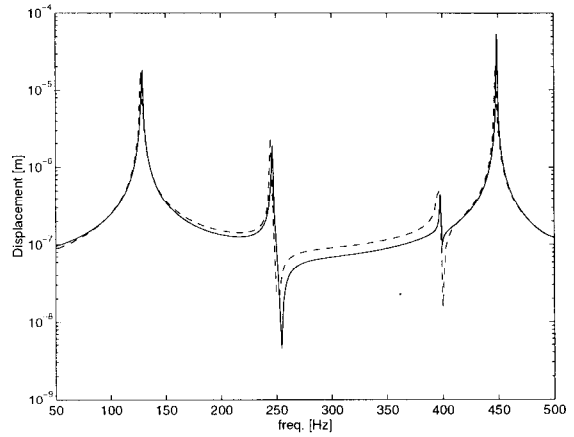
Fig. 4. Test case 2, frequency response to
actuator voltage input
Solid line - Lagrange model
Dashed line - FEM
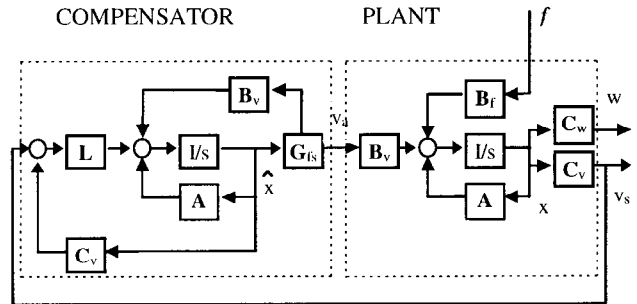
Fig. 5. Block diagram of the actively controlled system.
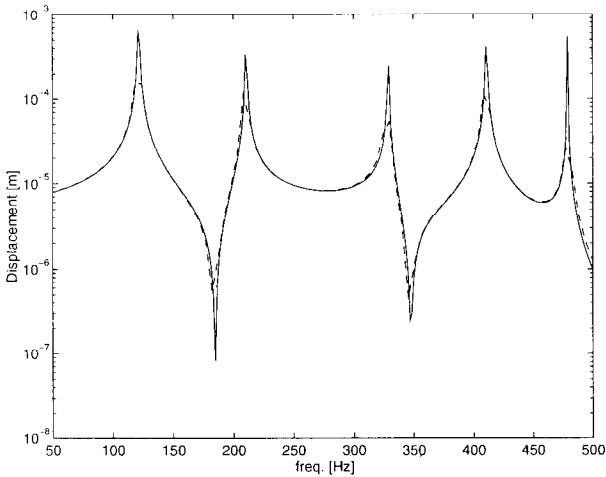
Fig. 3. Test case 1, frequency response to point force input
Solid line - Lagrange model
Dashed line - FEM
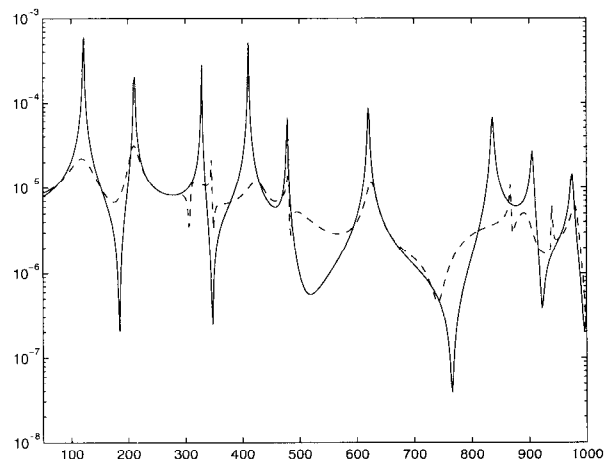
Fig. 6. Frequency response to point force
Solid line - Uncontrolled system
Dashed line - Controlled system